Supporting Information for "Observation of Ultrafast Vibrational Energy Transfer in Fibrinogen and Fibrin Fibers"

Biplab Dutta, [*,†] *Bart E. Vos,* [‡] *Yves L. A. Rezus,* [§] *Gijsje H. Koenderink,* [‡] *and Huib J. Bakker* [*,†]

[†]Ultrafast Spectroscopy, [‡]Biological Soft Matter, AMOLF, 1098 XG Science Park, Amsterdam, The Netherlands.

[§]Hogeschool Inholland, Amsterdam, The Netherlands

1. Polymerization of fibrinogen

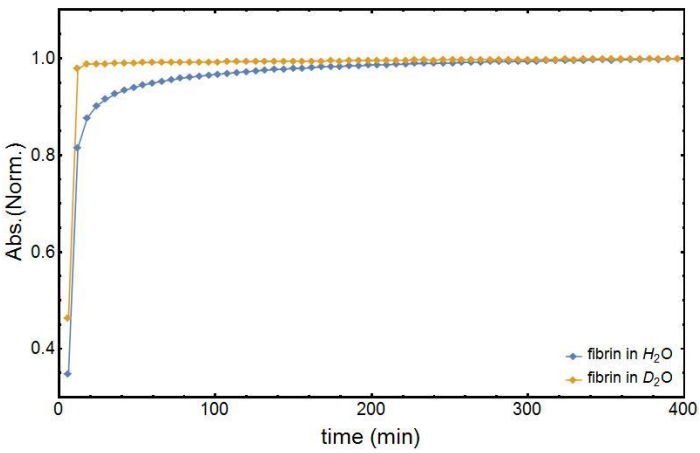

Figure S1. The progress of fibrin polymerization is monitored by measuring the rise in solution turbidity. The scattered light at a wavelength of 450 nm from fibrin gels in aqueous (H_2O) and in deuterated Tris buffer (0.5 M NaCl and 0.05 M Tris, pD =7.4) directly reports

the turbidity of the corresponding gels. The concentration of fibrin gels in both cases is 1 mg/ml. To visualize clearly the changes in turbidity, the absorbances at different times are normalized by the final absorbance at t=400 minutes.

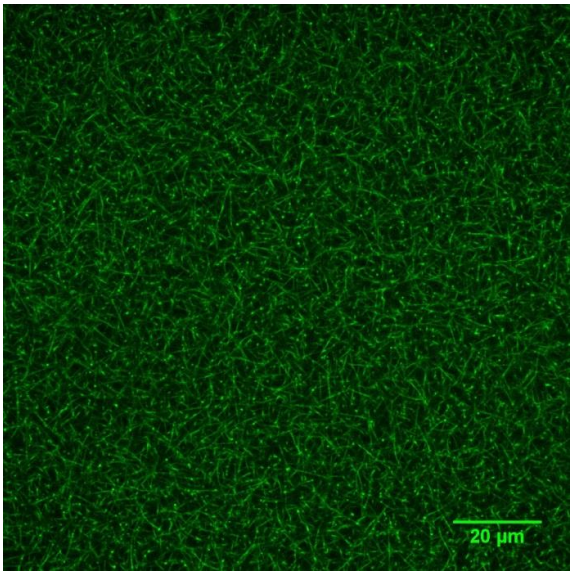

Figure S2. Confocal image of a fibrin gel (15 mg/ml) in deuterated Tris buffer (0.5 M NaCl and 0.05 M Tris, pD =7.4).

2. 2D IR spectroscopy

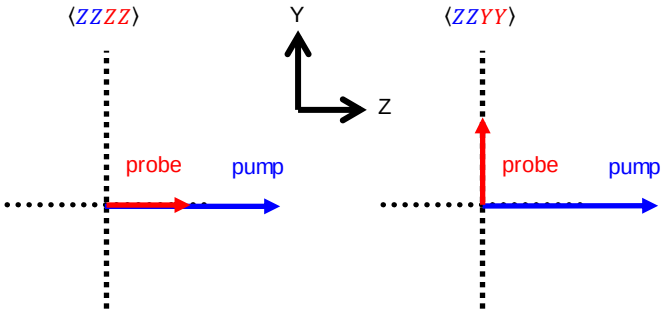

Figure S3. Schematic representation of ⟨ZZZZ⟩ and ⟨ZZYY⟩ configurations in the 2D experiment.[S1] The red and the blue arrows represent the polarization of the infrared pump and probe pulse respectively.

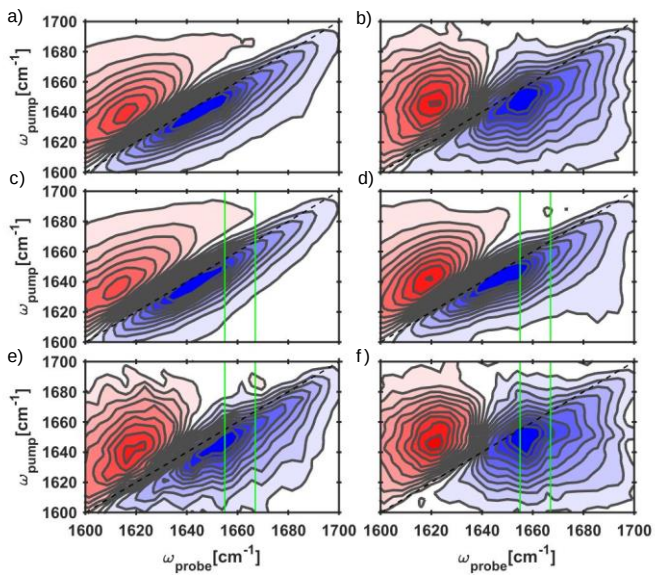

Figure S4. Isotropic 2D IR (⟨ZZZZ⟩ + 2⟨ZZYY⟩)/3 spectra of fibrin gels at a delay time of 0.3 ps (a) and 3 ps (b). The 2D IR spectra of fibrinogen in ⟨ZZZZ⟩ and ⟨ZZYY⟩ at 0.3 ps (c,d) delay and at 3 ps (e,f) delay. The ridge is represented by the green vertical grid lines around ω_{probe}=1660 cm^{-1}. Blue and red contours represent bleach and esa, respectively.

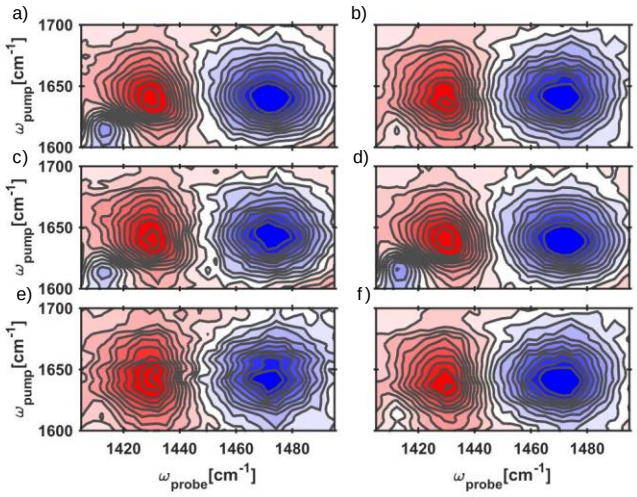

Figure S5. The 2D IR spectra of fibrinogen show the cross peaks between amide I′ and amide-II′ vibrational modes. Isotropic 2D IR (⟨ZZZZ⟩ + 2 ⟨ZZYY⟩)/3 spectra at 0.3 ps (a) and 2 ps (b). The 2D IR spectra of fibrinogen in ⟨ZZZZ⟩ and ⟨ZZYY⟩ at 0.2 ps (c,d) delay and at 2 ps (e,f) delay. Blue and red contours represent bleach and esa respectively. In these cross peaks, a delayed ingrowth is not observed.

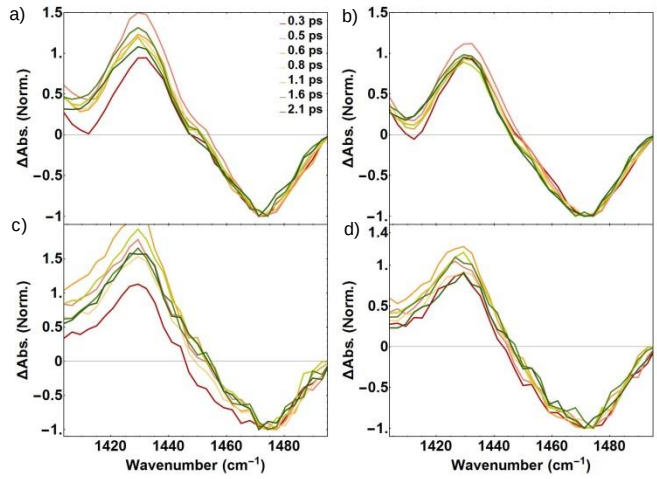

Figure S6. Slices taken through the 2DIR spectra of fibrinogen shown in Fig. S5 for ω_{pump}=1627 cm^{-1} (a,b) and ω_{pump}=1680 cm^{-1} (c,d). Clearly, no noticeable ingrowth is observed from these slices. Also, the ⟨ZZZZ⟩ (a,c) and ⟨ZZYY⟩ (b,d) 2D IR spectra at different time delays are barely distinguishable. Every slice is normalized by the corresponding bleach signal. The time delays are displayed in the legends and the absorption change, which is measured in 2D IR, is denoted by ΔAbs.

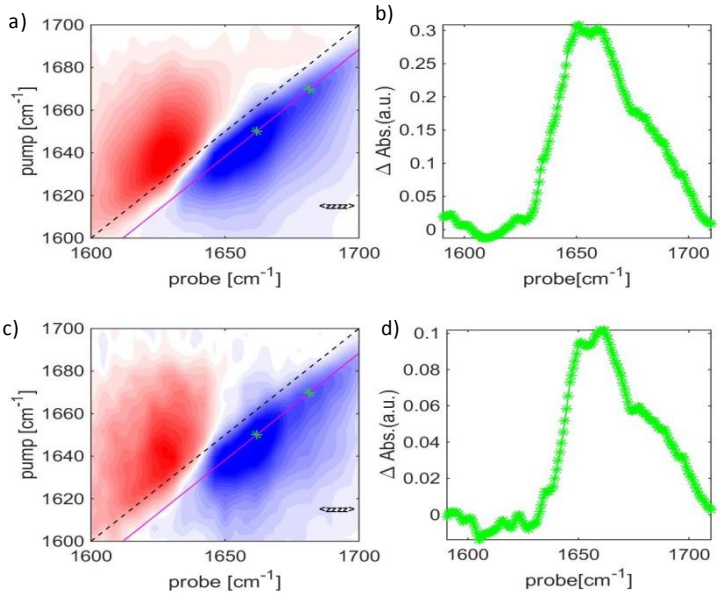

Figure S7. Diagonal slices taken through the 2D IR spectra of fibrinogen in ⟨ZZZZ⟩ for T_w=3 ps (a,b) and T_w=4 ps (c,d). Clearly, no significant effect of scattering is noticeable.

3. Kinetic Modeling

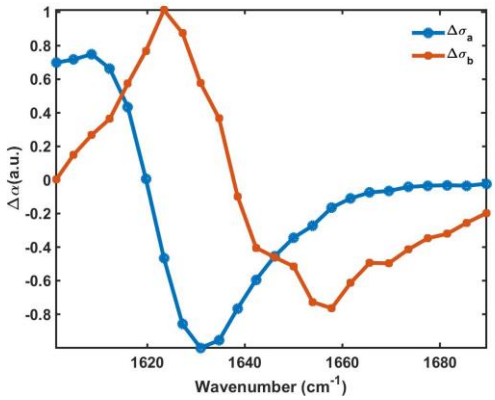

Figure S8. The transient spectra signatures $\Delta\sigma_a(\omega)$ and $\Delta\sigma_b(\omega)$ for fibrin gels obtained by fitting the isotropic 2D IR signals.

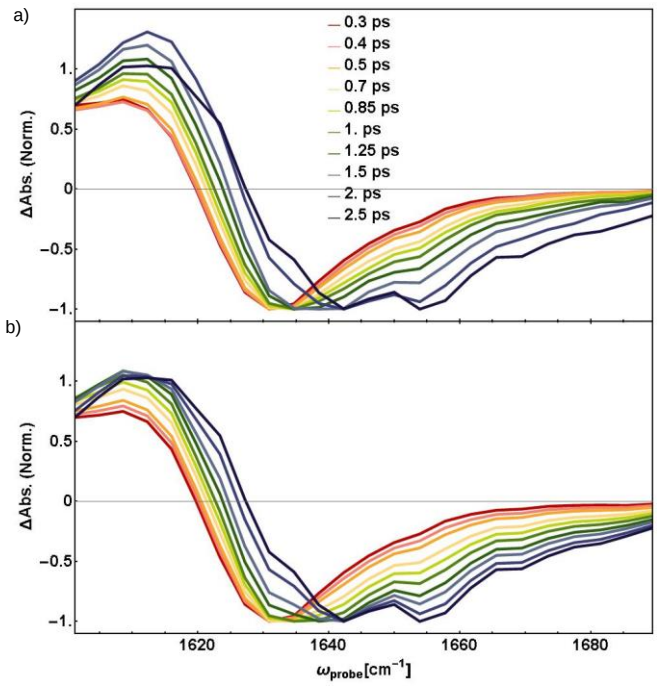

Figure S9. (a). Ten representative slices are taken from isotropic 2D IR spectra at ω_{pump}=1627 cm^{-1} of fibrin gels. The fitting of the experimental data (a) using the kinetic model is shown in (b).

4. Anisotropy calculation

The anisotropy (R) of the cross peak[S1] is defined by, $R=\frac{\langle ZZZZ\rangle-\langle ZZYY\rangle}{\langle ZZZZ\rangle+2\langle ZZYY\rangle}$

In Fig. S11, we show the anisotropy of poly-L-lysine dissolved in D_2O when it adopts an anti-parallel β-sheet conformation. Clearly, R=-0.16 is obtained from Fig. S10. It must be noted that the calculation of anisotropy here is straightforward due to the existence of isolated cross peaks. However, in our case, the interference of the diagonal peaks with the cross peaks hinders such a straightforward approach. In order to extract the information about the cross peak in such cases, one must remove the contribution of the diagonal peaks. By modeling our spectra, we have extracted the ingrowth part. Using this knowledge for the early delay spectra, the anisotropy parameter could be estimated. In our case, however, the normalization factor of the spectral slices must be taken into account; otherwise, the ⟨ZZZZ⟩ and ⟨ZZYY⟩ would weigh differently. As a consequence, the magnitude and the sign of R would differ drastically from the real value. For example, normalization of the datasets shown in Fig. S9 by the absolute values of corresponding bleach signals would make R=-0.42. Thus the inclusion of appropriate normalization factors (which is used to normalize our data in Fig. S9) into polarization dependent $\Delta\sigma_b(\omega)$ (Fig. S10), we obtain R=+0.3.

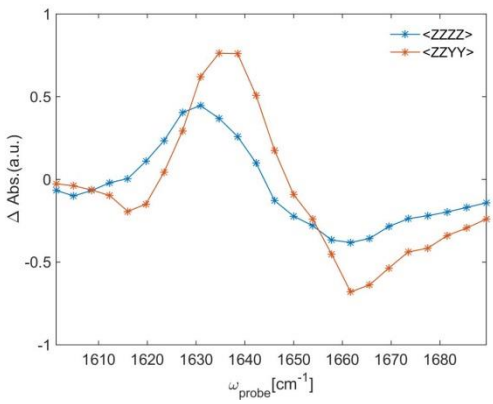

Figure S10. The spectral signature of $\Delta\sigma_b(\omega)$ for fibrinogen in ⟨ZZZZ⟩ and ⟨ZZYY⟩ polarization combination obtained by fitting corresponding polarization dependent signals.

Clearly, the anisotropy in our samples is different from a typical anti-parallel β-sheet conformation. Such drastic difference appears due to the fact that we probe energy transfer between a β-sheet mode and another mode that probably comes from turns.

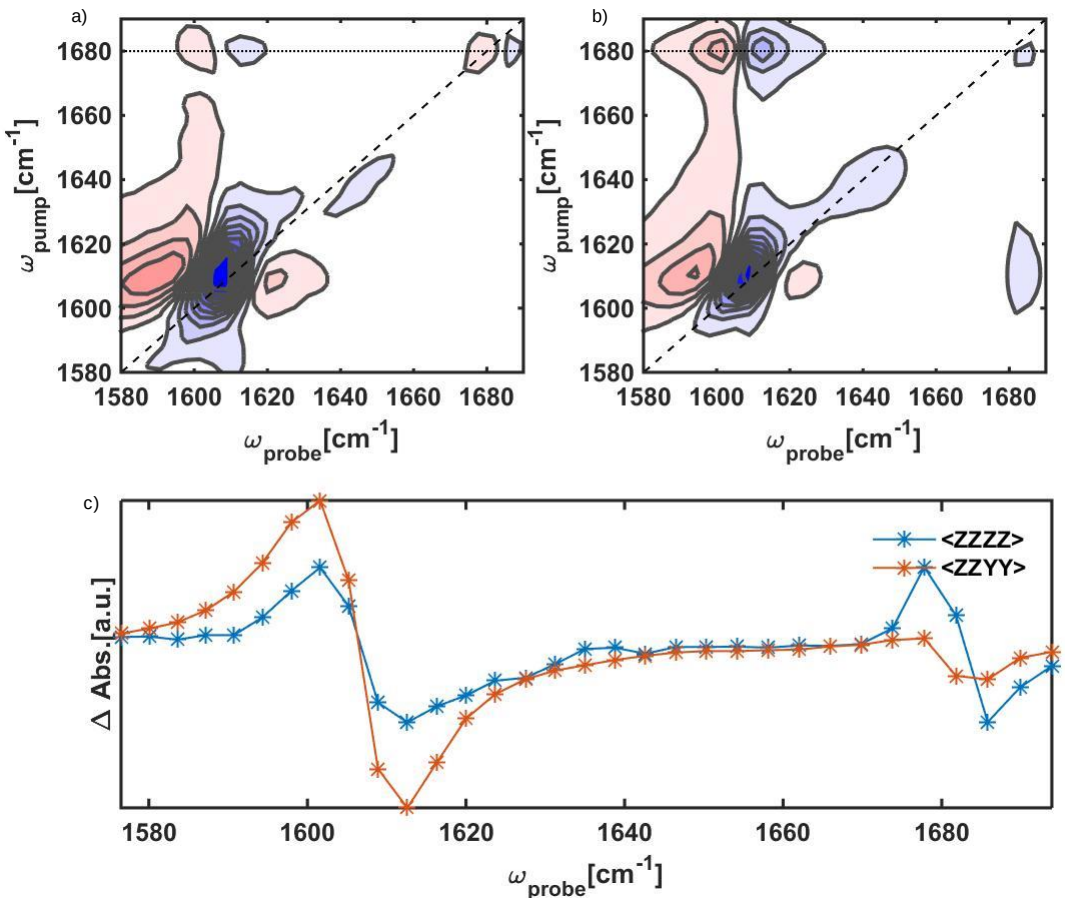

Figure S11. 2D IR spectra of poly-L-Lysine (at pH 12 and at 50°C) at 0.3 ps delay for ⟨ZZZZ⟩ (a) and ⟨ZZYY⟩ (b) polarization combinations. The anisotropy of the cross peak at ω_{pump}=1680 cm^{-1} is marked by differential contrasts in (a) and (b). A horizontal slice along of fibrin ω_{pump}=1680 cm^{-1} further illustrates the cross peak anisotropy clearly (c).

Reference

(S1) Hamm, P.; Zanni, M. T. *Concepts and Methods of 2D Infrared Spectroscopy*; Cambridge University Press: Cambridge, U. K., 2011.